Proc. CMP-MIC, pp. 395-402, Santa Clara, CA, March 2001.

A Fixed Abrasive CMP Model

Brian Lee[+], Duane S. Boning[+], Laertis Economikos[*]
[+]Microsystems Technology Laboratories, MIT, Room 39-567, Cambridge MA 02139
[*]IBM Corporation, East Fishkill Facility
Email: lee21@mtl.mit.edu

ABSTRACT

Chemical mechanical polishing (CMP) has emerged as the planarization technique of choice in both front-end (STI) and back-end (ILD) integrated circuit manufacturing. Conventional CMP processes utilize a polyurethane polishing pad and liquid chemical slurry containing abrasive particles. More recent work has examined the use of a fixed abrasive CMP pad [1], in which abrasive material is embedded into the polishing pad and released during the polish. In this work, we present a closed form fixed abrasive CMP model derived using step-height and fixed abrasive-specific pattern density dependencies. We then propose a methodology for characterization and calibration of the model, and compared the model prediction to experimental data.

INTRODUCTION

The current use of dielectric CMP in semiconductor fabrication processes benefits from analytical models that can be used as predictive and diagnostic tools for the CMP process. Recent work in the modelling of pattern dependencies in dielectric CMP processes has resulted in the formulation of several compact analytical models [4,5]. These models have been shown to produce a reasonable fit to experimental data for conventional CMP processes.

Stine [4] formulated an analytical model based on the concept that pattern density has a dominant effect on the post-CMP thickness of films. The basic idea is to incorporate pattern density into Preston's glass polishing equation and then integrate the resulting differential equation to create the set of model equations. The Stine model states that when removing the initial raised areas of the film, the removal rate of this *up area* is inversely proportional to the effective pattern (feature) density. The regions between the up areas (the *down areas*) do not polish at all in the initial stages. Once the raised areas are completely removed (i.e., a step height of zero is reached), the down areas begin to polish, and the up and down areas polish at the blanket (unpatterned) film removal rate.

In the Stine model, a key concept is the length scale over which the pattern density is calculated. Ouma [7] showed that a CMP process (specific combination of consumable set, tool, and process settings) is characterized by evaluating the distance (called the *planarization length*) over which the topography around a particular point affects the removal rate at that point. Using the planarization length to evaluate effective pattern density, along with the Stine model, it is possible to predict the post-CMP thickness of patterned films.

Burke [6] conjectured that the removal rate of the up and down areas varies linearly with the step height of the film. Grillaert [3] noted that this only occurs below a certain step height (the

(a)

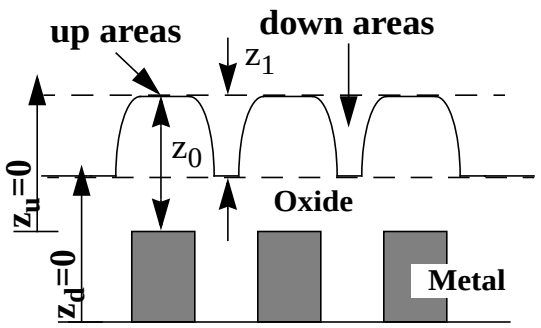

z: dielectric thickness at time t
z_0: initial dielectric thickness
z_1: initial dielectric step height
h_1: contact height (at contact time t_c)
K: blanket dielectric removal rate
t: polish time
ρ: effective pattern density
AR_u: amount removed in up area
AR_d: amount removed in down area

(b)

$$z_u = z_0 - \left(\frac{Kt}{\rho_0(x,y)}\right) \qquad z_d = z_0 \qquad \text{for} \qquad z \geq z_0 - z_1$$

$$z_u = z_0 - z_1 - Kt + \rho_0(x,y)z_1 \qquad z_d = z_0 - Kt \qquad \text{for} \qquad z < z_0 - z_1$$

(c)

$$AR_u = t_c\frac{K}{\rho} + K(t - t_c) + (1-\rho)\frac{h_1}{\tau}\left(1 - e^{-\frac{(t-t_c)}{\tau}}\right)$$

$$AR_d = K(t - t_c) - \rho\left(\frac{h_1}{\tau}\right)\left(1 - e^{-\frac{(t-t_c)}{\tau}}\right)$$

Figure 1: (a) Illustration of a typical dielectric film, before CMP; (b) The Stine dielectric CMP model (from [4]); (c) The Smith time-density dielectric CMP model (from [5]).

contact height). The effect is attributed to the surface compressibility of the pad. Smith [5] integrated this effect into the Stine model to create a more accurate model. The Smith model shows an improvement in prediction for low density features while keeping the same benefits of the density dependent modeling and characterization methodology.

MODEL DERIVATION

We now derive a CMP model based on the models discussed above. Removal rate diagrams, previously introduced for copper CMP modeling [2], are used to capture the effect of step height and pattern density on removal rate both graphically and in equation form. Dielectric CMP processes are modelled in two phases: polish before the pad contacts the down area between features (Phase 1) and polish after down area contact (Phase 2). The removal rate diagram is a plot of removal rate versus step height, and is used to capture the relationship between these two variables for the two phases of dielectric CMP.

The removal rate diagram for oxide CMP is shown in Figure 2. Phase 1 of the polish process is modelled with a constant up area removal rate as a function of step height, and a down area removal rate of zero. This captures the effect of the pad only contacting the up areas of the film. The up area removal rate for this phase has been conventionally modelled as being proportional to the blanket removal rate and inversely proportional to the effective pattern density [4]. For the current analysis, we shall denote the up area removal rate for Phase 1 as simply K_1, the patterned removal rate. Later in this work we will examine the relationship between K_1 and pattern density.

Phase 2 of the polish process is modelled as a linear decrease of the up area removal rate as a function of the step height, along with a corresponding linear increase in down area removal rate. This relationship was described in [6], and is based on Hooke's Law and the idea of pad compressibility. The up area and down area removal rates converge ultimately to the blanket removal rate K_2, when the step height is zero.

Models for conventional CMP processes have also assumed a distinct relationship between K_1 and K_2. For this analysis, we will decouple these two parameters, and assume no relationship. Later in this work we will discuss this issue and explain why it is best to approach the modelling this way with respect to the fixed abrasive CMP process.

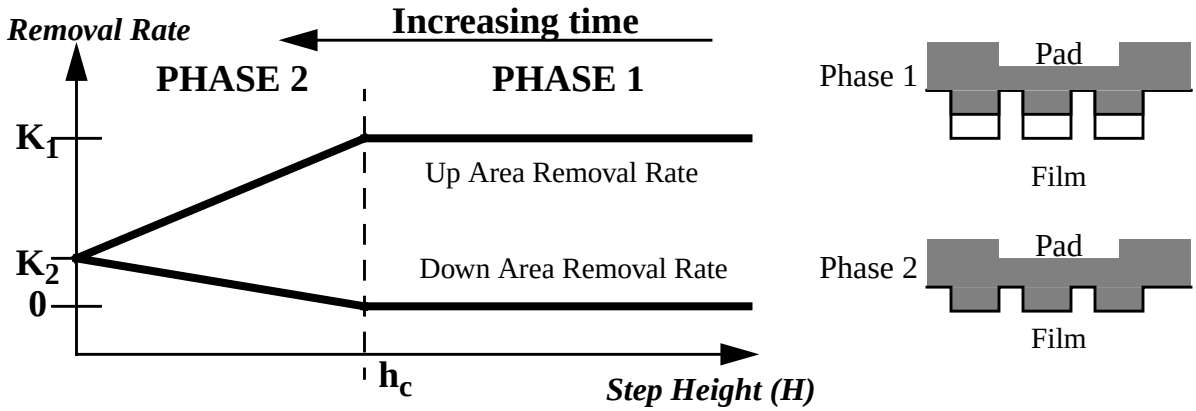

Figure 2: Removal Rate diagram for dielectric CMP polish. Phase 1 occurs between the initial polish and the time the pad initially contacts the down area. Phase 2 occurs between the end of Phase 1 and the planarization of the local step.

We next formulate equations for removal rate as a function of step height, consistent with the diagram of Figure 2. These can be integrated to derive analytic formulas for amount removed as a function of time. For Phase 1, the removal rates are independent of the step height:

$$RR_{up} = K_1 \qquad RR_{down} = 0 \qquad \text{(Equation 1a, 1b)}$$

The removal rates can be integrated directly to obtain formulas for the amount removed as a function of time for the up and down regions:

$$AR_{up} = K_1 t \qquad AR_{down} = 0 \qquad \text{(Equation 2a, 2b)}$$

The removal rates for Phase 2 can be expressed as functions of the step height, H:

$$RR_{up} = \frac{(K_1 - K_2)}{h_c} H + K_2 \qquad RR_{down} = -\left(\frac{K_2}{h_c}\right) H + K_2 \qquad \text{(Equation 3a, 3b)}$$

The difference of the removal rates in the up and down areas is equal to the rate of change of the step height with time:

$$\frac{dH}{dt} = -(RR_{up} - RR_{down}) = -\left(\frac{K_1}{h_c}\right) H \qquad \text{(Equation 4a, 4b)}$$

Note the sign convention; if the removal rate in the up area is greater than the removal rate in the down area, then the step height will decrease in time, hence the negative rate of change in the step height. This differential equation can be solved easily. We define a time t_c as the *contact time*, or the time at which the step height is h_c (the contact height), defined as $t_c=(z_1-h_c)/K_1$, where z_1 is the initial step height of the dielectric film. We then have the initial condition that at time t_c, the step height H is h_c, resulting in:

$$H = h_c e^{-\frac{(t-t_c)}{\tau_{ox}}} \qquad \text{(Equation 5)}$$

where τ_{ox} is the *oxide time constant*, and is equal to h_c/K_1. Substituting Equation 5 into Equation 3a and Equation 3b, we can derive expressions for the removal rate as a function of time:

$$RR_{up} = (K_1 - K_2)e^{-\frac{(t-t_c)}{\tau_{ox}}} + K_2 \qquad RR_{down} = K_2\left(1 - e^{-\frac{(t-t_c)}{\tau_{ox}}}\right) \qquad \text{(Equation 6a, 6b)}$$

It is then possible to integrate these equations to obtain expressions for the amount removed as a function of time:

$$AR_{up} = K_1 t_c + K_2(t-t_c) + h_c\left(1 - \frac{K_2}{K_1}\right)\left[1 - e^{-\frac{(t-t_c)}{\tau_{ox}}}\right] \qquad \text{(Equation 7a)}$$

$$AR_{down} = K_2(t-t_c) - h_c\frac{K_2}{K_1}\left[1 - e^{-\frac{(t-t_c)}{\tau_{ox}}}\right] \qquad \text{(Equation 7b)}$$

where τ_{ox} is the oxide time constant, equal to h_c/K_1. Note that density is not explicitly included in the equations at this point; we note that it is implicitly included in K_1, the patterned removal rate.

This model is generic enough to be applicable to a variety of CMP processes. It is particularly useful for modeling a fixed abrasive CMP process because it has been shown from previous experiments that the blanket removal rate is much smaller than the patterned removal rate, and that the usual inverse removal rate dependence on density may not be applicable.

REMOVAL RATE DENSITY DEPENDENCE

We noted earlier that in this model we purposely decouple the relationship between K_1, the patterned removal rate, and K_2, the blanket removal rate, in order to generalize the model. For fixed abrasive, this is particularly applicable. The classical relationship has been that K_1 is equal to K_2 divided by the pattern density. However, this does not appear to be the case for wafers polished here with a fixed abrasive ceria pad. It is not clear whether this is attributable to the ceria particles, or to the embedded fixed pad structure. We seek only to capture the combined effect for the consumable and process considered here.

To determine the relationship between K_1 and density, special test wafers were polished and data was taken for multiple polish times. Details of the experiment are described in the exper-

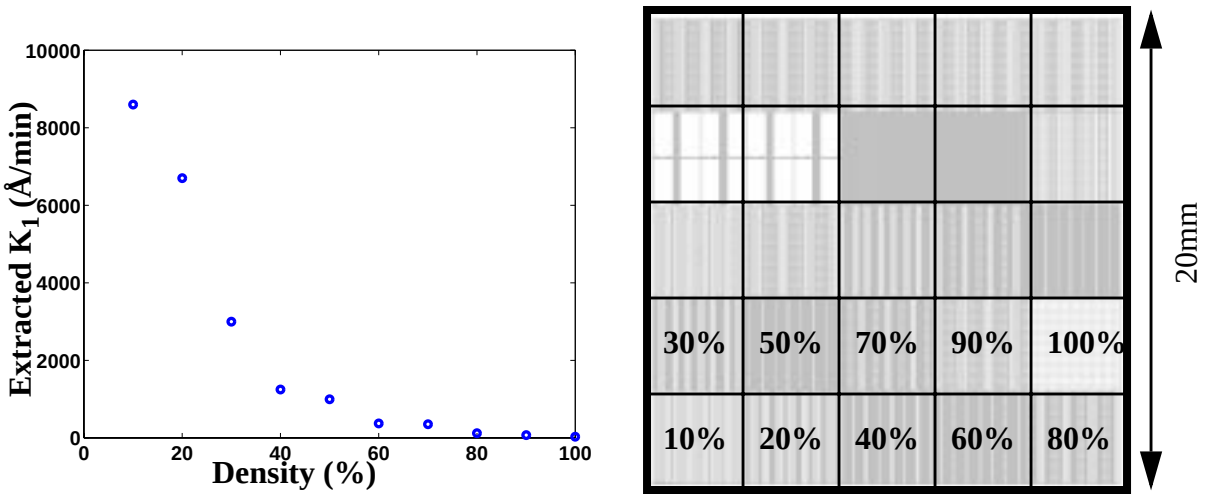

Figure 3: (a) Extracted K_1 as a function of density; (b) Experiment test mask. Numbers indicate local (drawn) pattern density.

imental data section later in this paper. The test pattern was a 20mm x 20mm die composed of 25 4mm x 4mm test structures of varying pitches and local pattern densities (as shown in Figure 3b). Measurements were taken at the center of test structures with different pattern densities, and removal rates were computed. A plot of removal rate versus local pattern density is shown in Figure 3a. We note that the local pattern density may not be equal to the effective pattern density; by using data from the center of the test structures, we hope to approximate the effective pattern density with the local pattern density.

Figure 4a illustrates the conventional CMP inverse density relationship between patterned removal rate and density, and compares it to the experimentally determined removal rates. The fitting parameter K was determined by optimizing for least root mean square (RMS) error to the experiment removal rates. As can be seen, the error is quite large, and there is significant underprediction for low density regions. Adjustment of the fitting parameter K to fit for low densities results in a large overprediction for the high density regions.

We conjecture that, for the certain consumable sets (such as the specific case of the fixed abrasive pad with ceria particles), the removal rate might exhibit an inverse relationship to density at low densities, but approaches a significantly lower removal rate at high densities. One functional form that fits this criteria is:

$$K_1 = \frac{K_\rho(1-\rho)}{\rho} + K_c \qquad \text{(Equation 8)}$$

Using this functional form, and optimizing the fitting parameters K_ρ and K_c for least RMS error results in a significantly better fit, as shown in Figure 4b. Note that the fitting parameter K_c in this equation should be equal to K_2, the blanket (100% density) removal rate.

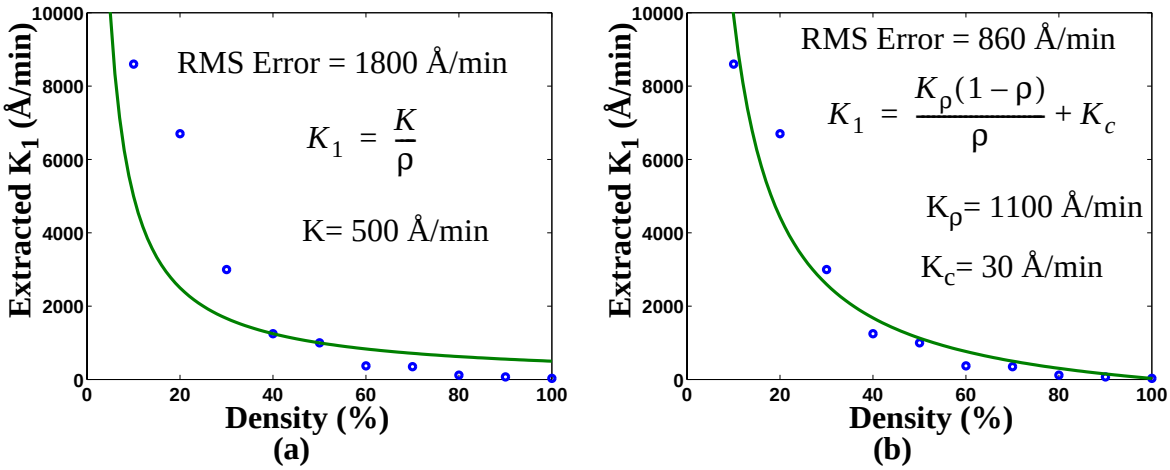

Figure 4: Functional relationships between pattern removal rate K_1 and density, compared to experimentally computed removal rates (a) pure inverse-density relationship; (b) proposed functional form.

CHARACTERIZATION METHODOLOGY

The characterization of a CMP process consists of an initial polish experiment using a special test mask (shown in Figure 3b), measurement of the polished test wafers, and calibration of the model parameters. Once the model has been calibrated, the model may be used in conjunction with an arbitrary layout to predict the final dielectric film thickness of a wafer processed using the same CMP process as the test mask. This characterization scheme is pictured in Figure 5.

The calibration of the model parameters consists of analyzing measurement data from the test wafers, performed on a particular CMP process, for several time steps. Measurement data is taken at the center of the each of the density structures for both up and down areas. The model parameter extraction first finds h_c and K_1; a single value of h_c and multiple values of K_1 (one for each density) are extracted by minimizing the RMS error of the model prediction to the measured data. The values of K_1 can be used directly (in a lookup table fashion), or used to extract the fitting parameters K_ρ and K_c in the functional form suggested by Equation 8. The parameter K_2 can be measured by polishing blanket wafers, or extracted simultaneously with the other model parameters as part of the error minimization fitting loop.

To extract the initial set of parameters, data is used from the center of the structures to minimize the effects of the planarization length on the effective density. After calibration of the initial model parameters, the planarization length of the process is extracted using additional measurement data taken closer to the edges of the structures. These additional points more strongly include the effects of neighboring structures, and thus are more effective for planarization length extraction. The planarization length is extracted by using the initial set of parameters and minimizing the error between the data and the model prediction, similar to the scheme described by Ouma [7].

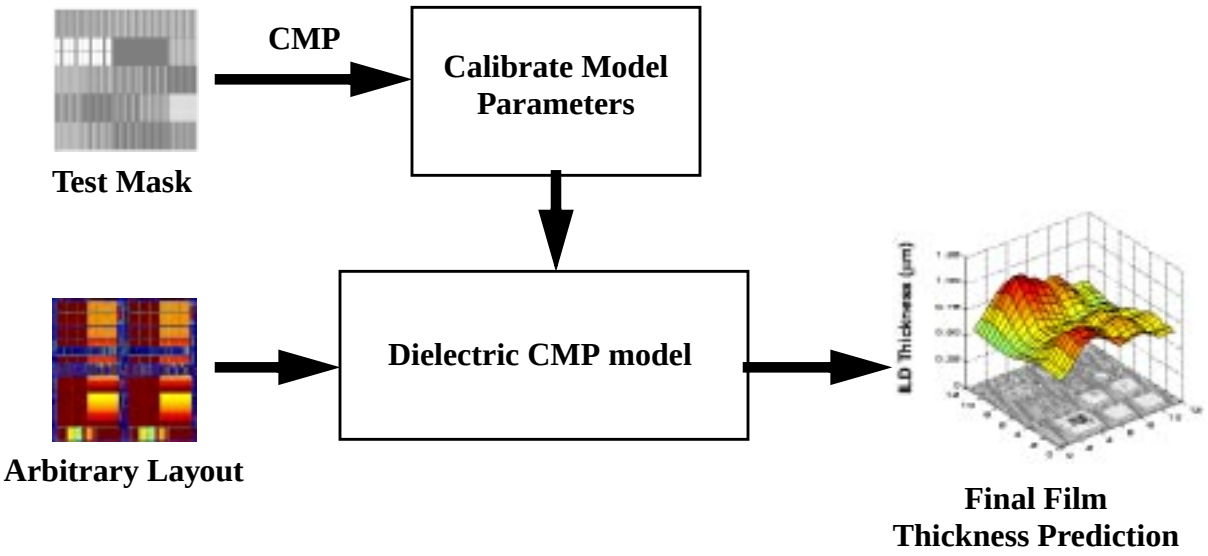

Figure 5: Dielectric CMP characterization and modeling methodology.

EXPERIMENTAL DATA

A set of STI wafers with the test pattern was run to test the model. These wafers had an STI trench depth of 3100 Å, a pad oxide of 60 Å, and a nitride thickness of 1100 Å. The dielectric used was HDP silicon dioxide, deposited to 4300 Å in the trenches. The actual dielectric step height that resulted was 3600 Å, as measured by profilometry scans. Wafers were processed on an Obsidian Flatland 501 CMP tool. A 3M fixed abrasive pad (SWR 159 std) was used, consisting of a top pad of ceria particles in a cylinder matrix, with a subpad stack of 60 mils of polycarbonate and 90 mils of foam. Eight wafers were processed at a pH of 11.5 for times of 20, 40, 60, 90, 120, 150, 180, and 210 seconds. The results of the experiment, as compared to the model prediction obtained using the calibration methodology (with K_1 determined via lookup table) is shown in Figure 6.

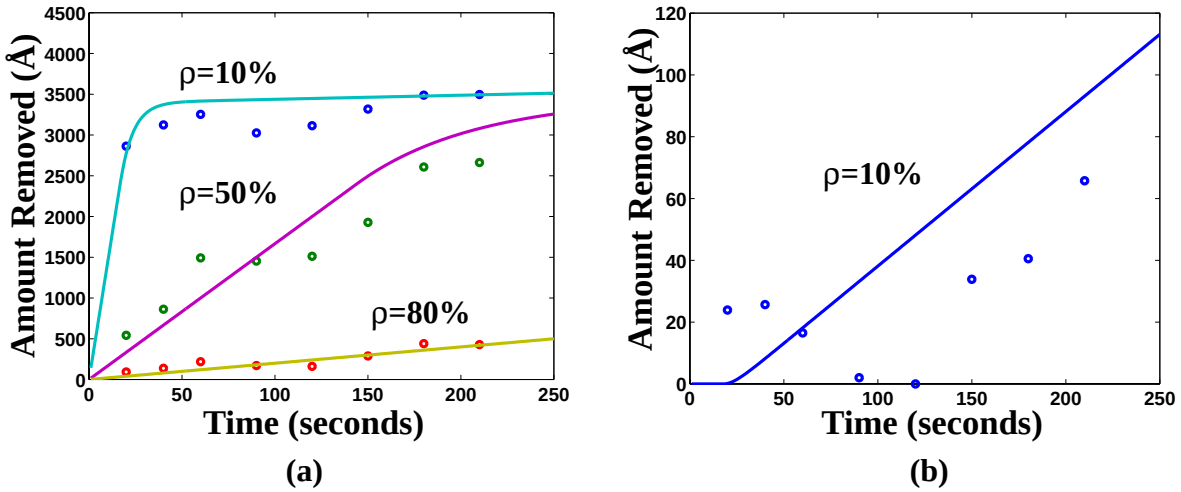

Figure 6: Experimental Data (o) vs. model prediction (-) for various pattern densities; (a) Up area prediction vs data;(b) Down Area prediction vs. data for 10%.

The general trend of the data is reasonably predicted by the model. The down area data for the 10% region is shown in Figure 6b; down area for the 50% and 80% region showed no appreciable polish, both in model and experimental data, for these regions. Table 1 shows the errors resulting from the prediction, and the extracted K_1 values used in the model. Other model parameters were a contact height of 1000 Å and a K_2 of 30 Å.

Table 1: Model parameter and errors for various densities

ρ(%)	K_1 (Å/min)	Up Area Error (Å)	Down Area Error (Å)	ρ (%)	K_1 (Å/min)	Up Area Error (Å)	Down Area Error (Å)
10	8600	223	30	60	375	140	10
20	6700	287	40	70	350	145	12
30	3000	374	24	80	120	60	7
40	1250	495	11	90	70	43	29
50	1000	355	15	100	30	27	n/a

CONCLUSION

We have derived a generic model for dielectric CMP processes, and described a characterization and calibration methodology for use with this model. We have demonstrated how the model can be used to predict the post-CMP film thickness of a fixed abrasive CMP process, and shown comparisons between the model predictions and experimental data. We have also examined the relationship between patterned removal rate and effective pattern density, and proposed possible functional forms for this relationship. For the specific case of shallow trench isolation CMP using fixed abrasive pads with ceria particles, the low blanket removal rate necessitates a very small overfill of the trench during deposition. This model can potentially be used to identify the maximum overfill to successfully planarize given a particular process window.

REFERENCES

[1] J. Gagliardi, *et al.*, “Total Planarization of the MIT 961 Mask Set Wafers Coated with HDP Oxide,” *Proc. CMP-MIC Conf.*, pp. 373-378, March 2000.

[2] T. Tugbawa, *et al.*, “A Mathematical Model of Pattern Dependencies in Cu CMP Processes,” *Proc. ECS Meeting*, pp. 605-615, October 1999.

[3] J. Grillaert, *et al.*, “Modelling step height reduction and local removal rates based on pad-substrate interactions,” *Proc. CMP-MIC Conf.*, pp.79-86, February 1998.

[4] B. Stine, *et al.*, “A Closed-Form Analytic Model for ILD Thickness Variation in CMP Processes,” *Proc. CMP-MIC Conf.*, pp.266-273, February 1997.

[5] T. Smith, *et al.*, "A CMP Model Combining Density and Time Dependencies," *Proc. CMP-MIC Conf.*, pp. 97-104, February 1999.

[6] P. Burke, *et al.*, “Semi-empirical modeling of SiO_2 chemical-mechanical polishing planarization,” *Proc. VMIC Conf.*, pp. 379-384, June 1991.

[7] D. Ouma, *et al.*, "An Integrated Characterization and Modeling Methodology for CMP Dielectric Planarization," *Proc. IITC Conf.*, pp. 67-69, June 1998.